

# Revue des Composites et des Matériaux Avancés-Journal of Composite and Advanced Materials

Vol. 35, No. 1, February, 2025, pp. 183-195

Journal homepage: http://iieta.org/journals/rcma

# **Evaluation of Thermo-Mechanical Properties of Iraqi Ceramic Materials and Their Modeling for Rotary Cement Kiln Using ANSYS Software Package**



Hamed A. Al-Falahi<sup>1\*</sup>, Ahmed Anees Alani<sup>2</sup>, Drai Ahmed Smait<sup>3</sup>, Mustafa B. Al-Hadithi<sup>4</sup>

- <sup>1</sup> Department of Chemical and Petrochemical Engineering, University of Anbar, Ramadi 31001, Iraq
- <sup>2</sup> Department of Civil Engineering, University of Anbar, Ramadi 31001, Iraq
- <sup>3</sup> Department of Medical Physics, Research Unit Centre, The University of Mashreq, Baghdad 10011, Iraq
- <sup>4</sup> Department of Chemical and Petrochemical Engineering, University of Anbar, Ramadi 31001, Iraq

Corresponding Author Email: h.alfalahi@uoanbar.edu.iq

Copyright: ©2025 The authors. This article is published by IIETA and is licensed under the CC BY 4.0 license (http://creativecommons.org/licenses/by/4.0/).

https://doi.org/10.18280/rcma.350120

Received: 19 September 2024 Revised: 30 October 2024 Accepted: 7 December 2024

Available online: 28 February 2025

#### Keywords:

bauxite, kaolin, refractory materials, cement kiln insulation, numerical analyses by ANSYS software package

# **ABSTRACT**

In order to raise the level of investment in local Iraqi resources, in this study, bauxite and kaolin ores were subjected to chemical and mineralogical analysis analysis to determine their suitability for the production of rotary kiln insulators. The results indicated that bauxite contains 63.02 wt% of alumina and 28.86 wt% of silica, which was reflected in the decrease in its softening point, while the mineralogical analysis showed the formation of mullite phase with a percentage of cristobalite, which was reflected in the increase in its specific gravity. The safe thermal temperatures of the firing program were determined by thermal microscope and DTA tests. The samples were produced according to the specification (DIN51053). The dry pressing was used with molasses as a binder. The samples were fired at 1300-1400°C. The effect of firing temperature, soaking time, particle size and forming pressure on the general properties of the produced insulator were studied. The results indicated that mixture (B) was characterized by ideal specifications compared to other samples. Based on the properties of the insulator, gases inside the rotary kiln, a numerical thermal analysis was performed in the unsteady state by simulating the ANSYS software package for each of the coal layer, the clinker layer, ceramic thermal insulator and the metal furnace wall. The results indicated that the ceramic insulator with a thickness of 50 cm is very suitable for insulating the rotary kiln without reaching the yield point of the furnace wall. Through the results, a database was reached as a guide for insulator designers to choose the best one to reduce effort and costs when dealing with practical applications.

#### 1. INTRODUCTION

The study of ceramic materials has attracted the attention of many researchers for more than a century, due to the great importance of these materials in many traditional ceramic industries such as cement, glass, and thermal insulators for furnaces [1]. Nano-silicon carbide helps in the formation of the glass phase with increased mullite formation which improves the mechanical properties of bauxite at 1400°C [2]. Particle size, consistency limits, and clay activity affect the composition and properties of clay to evaluate its suitability for structural ceramics and pottery [3]. An increase in temperature more than 1500°C and an increase in soaking time would increase the degree of phase transformation and decrease the value of the specific gravity of dense refractories [4]. Adding industrial aluminum oxide and two other types of Egyptian clay to the properties of refractories made from burnt bauxite reduces thermal expansion and increases the tolerance of the produced refractories against deformation that occurs at high temperatures [5]. The greatest secondary expansion in high-alumina refractories occurs when the percentage of alumina reaches (70-75%), and this results from the formation of mullite, which builds a layer surrounding the corundum grains, which weakens the mechanical resistance and increases the amount of slag penetration as a result of the increase in the porosity percentage [6]. Mullite gives high refractory resistance, low creep rate, thermal expansion, low thermal conductivity, high chemical and thermal stability, and high mechanical resistance [7]. A study on improving the phesomechanical properties of clay firebricks by adding 20 wt.% bauxite was conducted on local Iraqi natural rocks. The results showed that porosity and tensile strength increased and density decreased at 1300°C [8]. The corrosion resistance and mechanical properties at high temperatures of different types of alumina-silica refractory bricks were studied, and the results indicated that the chemical composition and porosity of the bricks are critical factors affecting the corrosion process and mechanical properties of refractory bricks [9]. Zirconia as a refractory additive increases resistance to both thermal shock, slag, wet fusion and hardening [10]. Other study focused on the Jordanian bauxite mineral, which included chemical and

mineralogical tests [11]. Another study was conducted to improve the properties of Iraqi bauxite by adding zirconia in percentages (5-20%) and concluded that it can be used at high temperatures [12]. Improving some of the properties of bauxite, attapulgite, CaO, and white cement using a weight percentage of 40% of gum arabic was also studied at temperatures (1350-1450°C). The results concluded that the properties of the refractories produced conform to the approved international standards [13]. It was found, through a study of the use of kaolin and metakaolin with some additives such as SiC and firebrick, that the bulk density and shrinkage of samples increased when the sintering temperature increased from 1100°C to 1500°C, while the open porosity of all samples decreased [14]. There is a study conducted on Iraqi bauxite as a thermal binder, in which the highest resistance to compression, bonding, and thermal shock was recorded at a burning temperature of 1450°C [15]. The balance between thermal insulation properties and porosity of refractory bricks made from bauxite and metakaolin is extremely important. The results at 1200°C indicated that increasing the porosity is undesirable, due to the increased absorption of liquids and gases and therefore the decrease in the bonding between the structural particles of the mortar [16]. The results of a comparative study of the microstructure, thermo-mechanical properties and corrosion resistance of refractory castings made of bauxite and corundum showed excellent stability and resistance to infiltration during corrosion due to smaller pore sizes and formation of a dense protective layer [17].

The present study focused on evaluating the properties of Iraqi refractory bricks made of bauxite and kaolin, and their suitability as ceramic thermal insulators for rotary cement kilns, and then conducting a numerical thermal analysis of the rotary kiln using the finite element method (FEM) through simulating the ANSYS software package in order to design a database that helps insulator designers to reduce effort and costs when dealing with those practical applications..

#### 2. EXPERIMENTATION

#### 2.1 Material evaluation and sample preparation

Several samples of local ceramic raw materials of kaolin and bauxite type were brought by the General Geological Survey, which is based on the deposits found in the area of 160 kilometer in the western desert of Iraq and were in the form of large-sized rock masses as shown in Figure 1(a). Bauxite is the natural ore from which most alumina is made. The ore consists of gypsite (Al(OH)<sub>3</sub>), bohemite ( $\gamma$ -AlO(OH), and diaspore ( $\alpha$ -AlO(OH) with a little hematite, which is iron ore. Kaolin is a type of fine, soft, white rock, which consists mostly of the mineral kaolinite (hydroxylated aluminum silicate Al<sub>2</sub>(OH). (4Si<sub>2</sub>O<sub>5</sub>) as shown in Figure 1(b). Molasses is a high-viscosity, dark-colored organic substance. It was used at a rate of 0.5% as a binder. After burning, it also leaves voids that contribute to increasing porosity.

As a first stage, a quantity of raw bauxite was burned in order to reduce the rate of volumetric shrinkage and obtain grog at a rate of 5°C/min until a temperature of 500°C, and then heating at a rate of 10°C/min until a temperature of 1000°C. Then come the crushing, grinding, and sieving operations using a group of American screens of different sizes, for both burnt and unburned ore. Because burnt bauxite is a refractory material with little plasticity, It has been suggested to add some kaolin and unburned bauxite with a granularity of

(< 0.18 mm) as a binder that facilitates the shaping process and increases the cohesion of the produced samples. The materials are mixed for the mixtures using an electric mixer to ensure homogeneity of the mixture. Table 1 shows the weight percentages of the mixtures proposed in the study to demonstrate the effect of different particle sizes and operational conditions on the insulator produced.

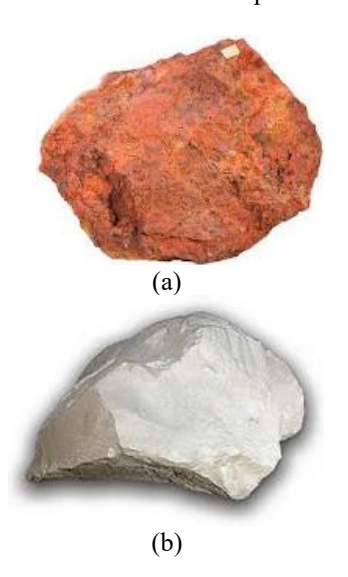


Figure 1. (a) Bauxite ore, (b) Kaolin ore

Table 1. Weight ratios of raw materials for mixtures

Sample	Grog Bauxite (wt%)		Unfired Bauxite (wt%)	Unfired Kaolinite (wt%)		
No.	< 0.5 mm 40%	0.5-1 mm 20%	1-2.8 mm 40%	< 0.18 mm		
A		90		5	5	
В		80		10	10	
C		70		15	15	
D		60		20	20	

The second stage of the study was based on the results of the first stage and the optimal practical conditions that were reached, taking into account the best mixing ratio, granularity, formation pressure, soaking time, and burning temperature. It was found that mixture (B) achieves the best specifications, and based on it was chosen as the best model.



Figure 2. Product specimen

Cylindrical samples were prepared as in Figure 2, with a length of 30 mm and a diameter of 30 mm, according to the German standard DIN51053 [18]. The amount of water added was 10% and the amount of molasses was 1% of the total weight of the sample as a binder. The semi-dry pressing

method was used using an Instron programmed compression and tensioning device with a loading force of 10 KN/min and a pressure of 40 N/mm<sup>2</sup>.

The samples were left for 24 hours in the laboratory atmosphere, then dried at a temperature of 60°C for 60 minutes and at 110°C for 24 hours, as the ceramic material shrinks slightly when dried.

In the first stages of drying, the molecules of the material are surrounded and separated from each other by a thin film of water, and during drying removes water and the boundaries of separation between molecules decrease, which leads to shrinkage. It is important to control the amount of water removed during drying to prevent any deformations in the dried body. Therefore, the evaporation rate must equal the rate of water diffusion from the inside to the surface, and this is done by controlling the drying rate [19].

The burning program was proposed based on the results of differential thermal analysis (DTA) and thermal microscopy by observing the changes that occurred to the raw bauxite at different temperatures. Different temperatures were selected ranging from 900-1400°C. The firing process of the samples was carried out in a programmed electric furnace under a noninert atmosphere up to 1400°C after the samples were placed inside the furnace on a layer of alumina powder to avoid adhesion and chemical reaction with the oven base. A burning program was initially reached, consisting of four stages:

- Raise the temperature at a rate of 2°C/minute from laboratory temperature to 700°C.
- Raising the temperature at a rate of 3°C/minute from a temperature of 700°C to a temperature of 1000°C.
- Burning continued at a rate of 3°C/minute from the temperature 1000°C until the final temperature, then the specimens were left at this temperature for a soaking time of two hours in order to increase the sintering efficiency.
- The cooling stage, which begins with the end of the soaking time and the programmed oven stops working. The samples are left after the oven stops for 24 hours, thus making them ready to determine their general properties.

The general properties of the produced samples were determined in terms of degrees of firing temperature. Comparing the results and the extent to which they are affected by changes in grain size, soaking time, and additives. The weight change and the permanent linear change were measured according to the following equation [20].

$$PLC\% = \frac{L_1 - L_2}{L_1} \times 100\%$$
 (1)

Bulk density was measured according to the American standard method ASTMC20 with the following relationship [19];

$$\rho = \frac{W_D}{V} \tag{2}$$

Porosity was measured using the Rosca device according to the Cobb method. In this method, the volume of the solid fraction (VS) and the total volume of the sample (Vt) are measured, and through this we can determine the volume of pores ( $V_P$ ) as;

$$Q = \frac{V_t - V_s}{V_t} \times 100 = \frac{V_p}{V_t} \times 100$$
 (3)

Water absorbtion was measured according to the American standard method ASTM C20 [19];

$$W\% = \frac{W_S - W_D}{W_D} \times 100$$
 (4)

Specific gravity was measured according to the American standard method ASTM C20 [19];

$$T = \frac{W_D}{W_D - W_n} \tag{5}$$

Cold Crushing Strength was performed according to the American Standard Method ASTM C130-84 [21].

$$S = \frac{F}{A} \tag{6}$$

Thermal shock resistance was measured according to the German standard method DIN 51068 [22]. The thermal conductivity of the fired specimens was measured by the Disc Lee Conductivity Tester [23].

# 2.2 Devices description

In this study, XRD model PW1877 was used to perform chemical and mineralogical analysis of raw materials, heating microscope type IA. Ernest Leitz Gmbh, to identify the behavior of raw materials during heating from changes such as expansion, contraction and melting, differential thermal analysis device (DTA) to identify the thermal behavior of raw materials during heating or cooling as a result of chemical and physical changes, Zecker cone to measure softening point to know the safe temperature of the produced ceramic insulator, Furnaces at 1500°C, 250°C, Disc Lee for conductivity testing, laptop, laboratory glassware and ANSYS software package.

# 3. RESULTS AND DISCUSSION

# 3.1 Analysis of raw materials

The chemical components of the raw materials give an important indication of the nature and properties of the produced refractories. Table 2 shows that Iraqi raw bauxite burned at 1400°C contains an average percentage of alumina estimated at 63.02%, and due to the low percentage of alumina, its softening and melting point decreases. Bauxite also contains 28.86% silica. The white kaolin used as a plasticizer contains 34.45% alumina and 46.84% silica. The presence of silica in bauxite and kaolin helps in the formation of mullite by reacting with aluminum oxide at high temperatures, thus improving the density, specific gravity and resistance to sudden thermal chock [7, 13]. The high percentage of iron oxide in both types (raw and burnt), which may be reduced to (FeO) if burning takes place in an inert atmosphere and thus leads to a decrease in the overall softening point by increasing the rate of solid phase reactions which produce chemical compounds with low melting points. Iron oxide also gives a dark color to the produced refractories, which was observed when samples were burned to 1400°C. The percentage of fluxing materials in the raw kaolin is about 8.6% and these materials lead to a decrease in the softening point, as well as early deformation of the produced refractories [5, 11-12].

Table 2. The weight ratios of Iraqi raw materials

	Ra	aw Materi			
Chemical Comp.	Cal.	Raw	Raw	Standard Values	
%	Bauxite	Bauxite	Kaolin	Cal.	Raw
6:0	20.06	21.00	46.04	Baux.	Kao.
SiO <sub>2</sub>	28.86	21.88	46.84	10-45	50-60
$Al_2O_3$	63.02	56.78	34.45	50-90	25-45
Fe <sub>2</sub> O <sub>3</sub>	1.96	1.00	1.09	0-1	0-1
$TiO_2$	2.04	2.30	1.40	1-4	1-2
CaO	1.10	0.58	0.83	0-1	0-1
MgO	0.21	0.16	0.28	0-1	0-1
L. O. W.	0.05	15.59	12.64	-	-

# 3.2 Mineralogical analysis of raw materials

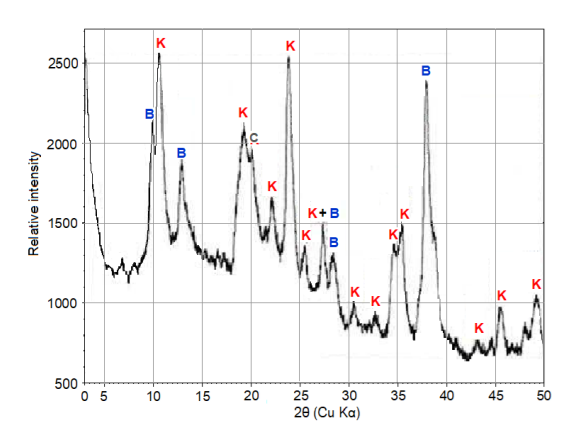


**Figure 3.** X-ray diffraction analysis of raw bauxite . (K) Kaolinite, (B) Boehmite, (C) Calcite

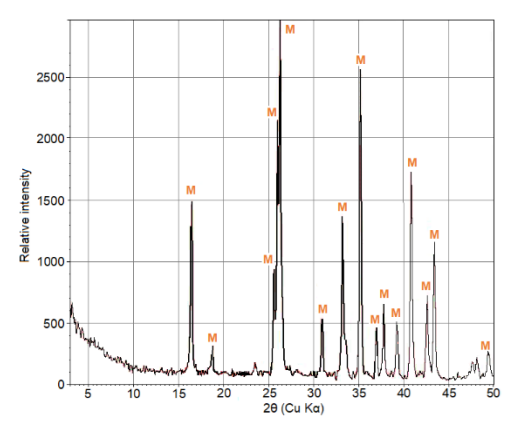


**Figure 4.** X-ray diffraction analysis of firing bauxite at 1400°C (Grog Bauxite), (M) Mullite

The mineral composition is affected by the chemical composition of the raw material and the burning temperature. The results of the X-ray diffraction analysis in Figure 3 for raw bauxite indicate the appearance of kaolinite, boehmite and small percentage of calcite, while for bauxite burned at 1400°C, the appearance of mullite is mainly observed with a small percentage of cristobalite. Mullite has a high specific gravity of about (3.02), which in turn leads to an increase in the specific gravity of the produced refractories as in Figure 4. On the other hand, the analysis of raw kaolin showed the highest percentage of kaolinite with a low percentage of quartz as shown in Figure 5.

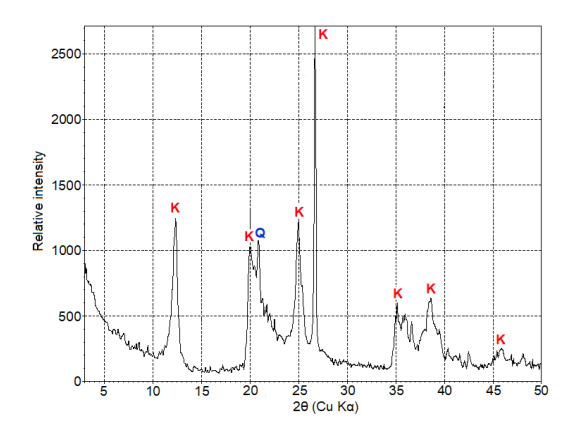


**Figure 5.** X-ray diffraction analysis of white kaolin. (K) Kaolinite, (Q) Quartize

# 3.3 Heating microscope test of raw materials

It was observed that the change that occurred to the bauxite and kaolin during the testing process at high temperatures up to 1500°C was within the permissible limits for refractory materials, which indicates that they are highly melting refractories. This result was adopted in determining the safe temperatures for the burning program 1400-900°C.

# 3.4 Differential thermal analysis of raw materials (DTA)

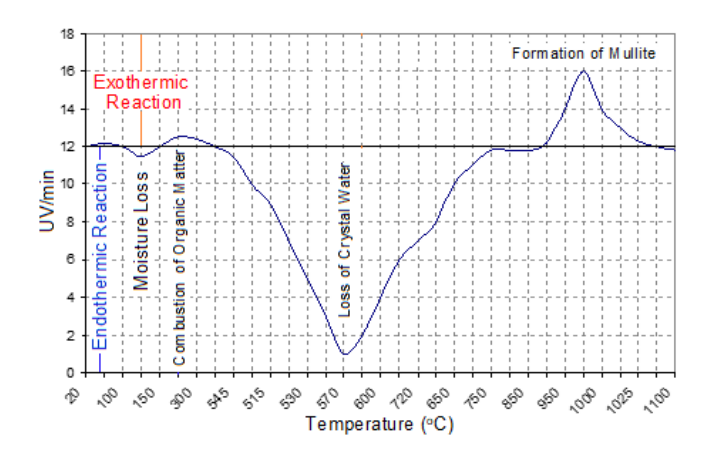


Figure 6. DTA test of raw kaoline

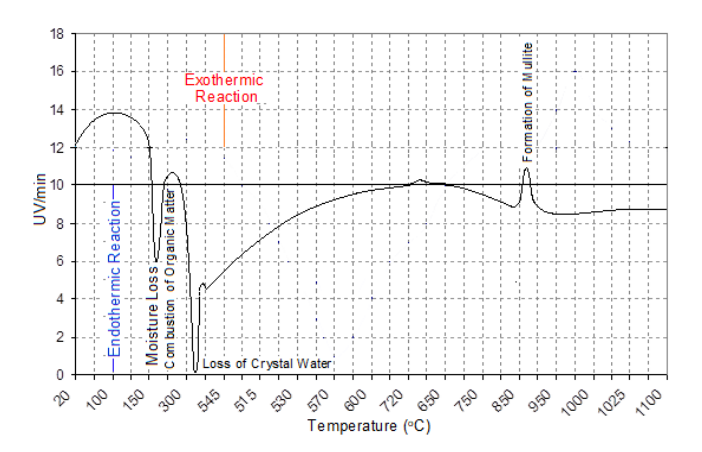


Figure 7. DTA test of raw bauxite

Through this analysis, the endothermic and exothermic reactions were determined. Figure 6 shows that the kaolin clay loses moisture at a temperature of 100-150°C, and there is

combustion of organic materials at around 300°C, then the stage of endothermic reactions begins, and crystal water is lost at around 566-580°C. Mullite is formed at a temperature of 970 -1000°C, which is an exothermic reaction [24]. Bauxite may lose moisture at 230°C, organic materials burn at around 300°C, its crystalline water is lost at 450°C, and mullite is formed at 912°C, as shown in Figure 7. To ensure complete and quiet loss of crystal water, and to solve the problem of cracking that may occur in the final product, and since bauxite and kaolin clay contain hydrated aluminum silicates, which completely lose their crystal water at around 550-600°C, a program was proposed to burn the specimens to ensure that sufficient time is given to the specimens to complete the chemical reactions. The oven temperature was raised at a rate of 2°C/min from the laboratory temperature to 700°C, which is the temperature at which no trace of crystal water remains, then burning continued at a rate of 3°C/min until reaching the required temperature.

# 3.5 Softening point test of raw materials

In order to ensure the resistance of raw materials to high temperatures, the softening point of kaolin and raw bauxite was tested with a Zeger Cone, which is the accurate method for measuring the melting point of refractories. It cannot be measured by traditional methods, because bauxite refractories are heavy ceramic materials, and the cohesion between its molecules is achieved through ionic and covalent cohesive forces and van der Waals forces [25], and each of these forces has energy, so the raw materials do not melt at the same time, and for this reason the Zeger method was used to determine the softening point, as the results showed that burnt bauxite can withstand more than 1650°C according to Zeger Cone No. 31, while white kaolin can withstand more than 1600°C, which is equivalent to Zeger Cone 23, The increase in softening point is attributed to the high percentage of alumina in the raw materials under study, as it has a melting point of 2050°C.

# 3.6 Effect of soaking time on the general properties of refractories produced at constant firing temperature

Soaking time refers to the period of time during which the refractory material remains at the required temperature for burning. The effect of this time will be reflected on its general specifications affecting thermal insulation, which is an important economic requirement for rationalizing energy in national industries. For this reason, a mixture (B) from Table 1 consisting of 10% Unfired Bauxite, 10% kaolinite and 80% Grog Bauxite was chosen. The reason for choosing it is that it contains a medium percentage of plastic material, and its clear and acceptable effect on the soaking time. An economic firinging temperature of 1200°C and a variable soaking time (0,1,2,3,4 hr) were chosen. From the results in Table 3, it was noted that the properties had a noticeable change up to a soaking time of two hours, and above this time there was stability in the properties or a slight change that was not taken into consideration, so this time was adopted for temperatures from 1000-1400°C for the next stage of the study, and it will be discussed in detail.

After the shaping stage, the specimens are wet and highly porous, which may reach 50% of the total volume. After the firing process, the weight and dimensions of the specimens decrease as a result of the reduction in pore sizes. This reduction increases with the increase in firing temperature and

the loss of crystal water. It should be noted here that all changes in the product must be completed during the manufacturing stage. The change in the percentage of the added plasticizer affects a group of important properties of the produced ceramic insulator.

**Table 3.** Effect of soaking time on general properties of the mixture (B) at constant firing temperature

	Soa	king Ti	Standard Values			
Prosperity						
	0	1	2	3	4	values
Comprehensive	25.	25.	26.	26.	26.	
Strength	<i>23</i> .	23. 7	20.	20. 4	20. 5	20-45
N/mm <sup>2</sup>	3	/	2	4	3	
Specific	3.7	3.7	3.8	3.8	3.8	2-5
Gravity	2	7	7	8	8	2-3
Water	11.	9.2	8.8			
Absorption	9	9.2 7	0.0 4	8.5	8.4	7-15
(%)	9	/	4			
Apparent	30.	26.	25.	24.	23.	15-30
Porosity (%)	8	8	3	0	4	13-30
<b>Bulk Density</b>	1.9	2.0	2.0	2.0	2.8	1.8-2.35
$(g/cm^3)$	9	1	3	5		
Permanent	4.3	4.6			5.7	
Liner Change	4.3 9	4.0 7	4.8	5.0		0-5
(%)	9	/			8	
Weight Change	1.6	1.6	1.7	1.7	1.7	
<b>(g)</b>	7	9	1	1	9	-
Thermal Shock					<b>\2</b>	
Resistance	7	<15	>20	>25	>2 5	>15
(cycle)					3	

As clay loses its water of association when the temperature is raised to 566-580°C, and bauxite at 450°C, then it loses its plasticity completely with the inability to return to the plastic state if it is wetted with water again. Organic materials and impurities decompose with the rise in temperature and the materials with relatively low temperatures melt, after which the materials with higher melting points melt, and a group of physical and chemical processes occur such dissolution. recrystallization, melting, crystallization, decomposition of compounds and formation of other compounds. All these changes lead to a difference in weight and increase with the increase in the proportions of the plastic phase in the mixture. This is shown in Figure 8, which shows that the change in weight increases with the increase in the proportions of the plastic material in the mixture and the increase in the burning temperature.

Figure 9 shows that the linear change increases with the increase in the proportion of raw kaolin in the mixture, which is a plasticizer. As this proportion increases and the temperature rises, the chemical reactions that occur increase, as compounds decompose and new compounds are formed, then changes occur in the volume and thus the product shrinks. The increase in the rate of reactions in the solid phase between oxides and impurities in the specimens results in compounds with a low melting point, which leads to an increase in the proportion of the liquid phase, which represents a good medium for the sliding of the particles over each other.

With the help of the surface tension of the liquid, the

dimensions of the specimen shrink. It must be noted that the change in dimensions remains close for all mixtures up to a temperature of 1200°C and increases significantly above this temperature. In general, it can be said that the amount of shrinkage is related to the plasticity of the ceramic material, as it increases with its increase and decreases with its decrease.

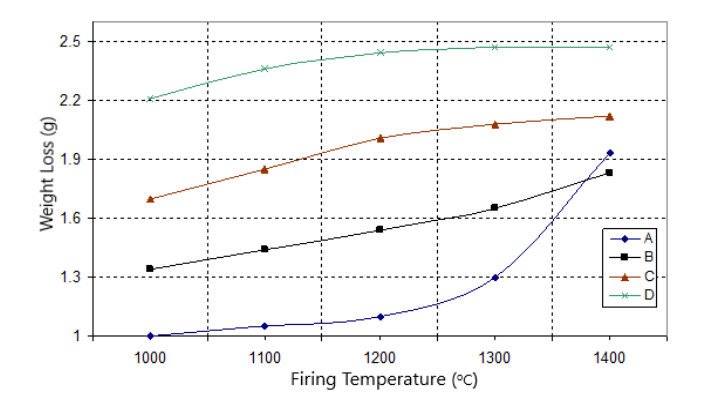
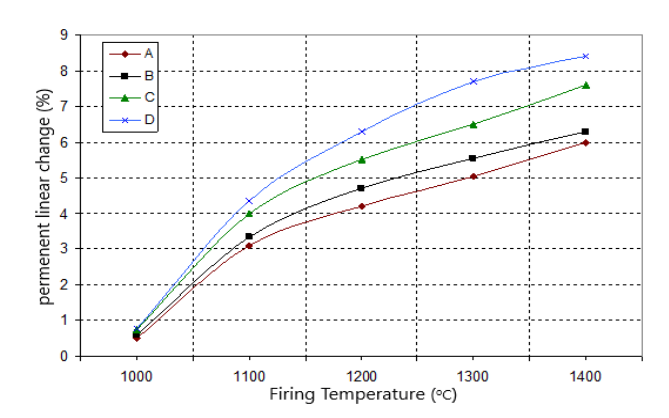
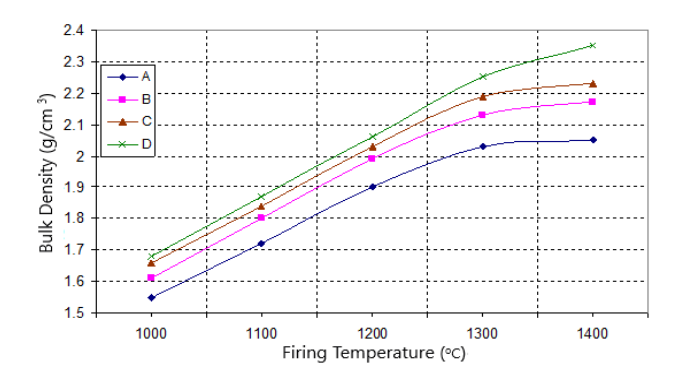


Figure 8. Effect of burning temperature on the weight loss



**Figure 9.** The effect of burning temperature on linear change of the produced specimens



**Figure 10.** The effect of burning temperature on the bulck density of the produced specimens

The results in Figure 10 show a significant increase in the bulck density with increasing firing temperature for all mixtures, due to the sintering process and the closeness of the grains, as well as the increase in the percentage of the liquid phase resulting from the chemical reactions between the oxides of the mixture, which are; SiO<sub>2</sub>, Al<sub>2</sub>O<sub>3</sub>, Fe<sub>2</sub>O<sub>3</sub>, CaO, MgO).

The specific gravity of the produced samples is greatly affected by the chemical and mineral components, firing temperature, and particle size. The oxides Al<sub>2</sub>O<sub>3</sub>, Fe<sub>2</sub>O<sub>3</sub>, CaO, and MgO in the prepared mixtures have high specific gravity

that is not affected by low temperatures. This is observed in Figure 11, where the specific gravity value of the mixtures fluctuates between 2.72 and 4.18 up to a temperature of 1200°C. When the temperature rises to 1400°C, a significant increase in the specific gravity value occurs. The above results are explained by the fact that increasing the temperature and the plasticizer ratio leads to an increase in the rate of reactions occurring between the components of the refractory material, which leads to an increase in the degree of transformation and the formation of products with high specific gravity, thus raising the value of the final specific gravity of the product.

Before the firing process, the refractory body is highly porous and most of the pores are in the form of open pores, but during the firing process, a portion of the open pores are reduced and transformed into closed pores, which is why the percentage of closed pores increases, but this percentage quickly decreases as the sintering process progresses and the firing process is completed. Figures 12 and 13 show a clear decrease in the apparent porosity and water absorption with increasing firing temperature for all granular sizes and all mixing ratios, due to the sintering process and the convergence of the granules, as well as the increase in the percentage of phase transformations, which results in an increase in the percentage of the liquid phase resulting from chemical reactions between the oxides that make up the mixture.

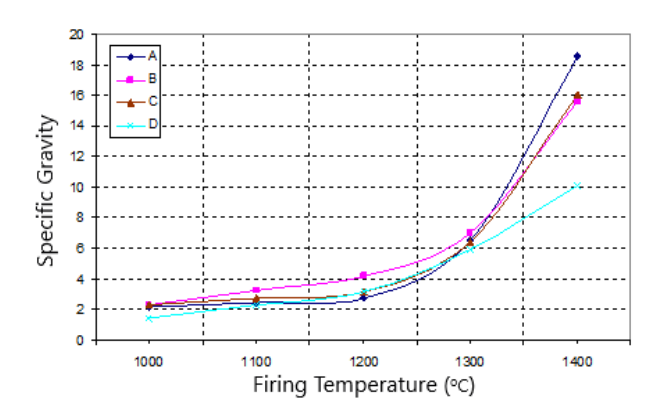


**Figure 11.** The effect of burning temperature on the specific gravity of the produced specimens

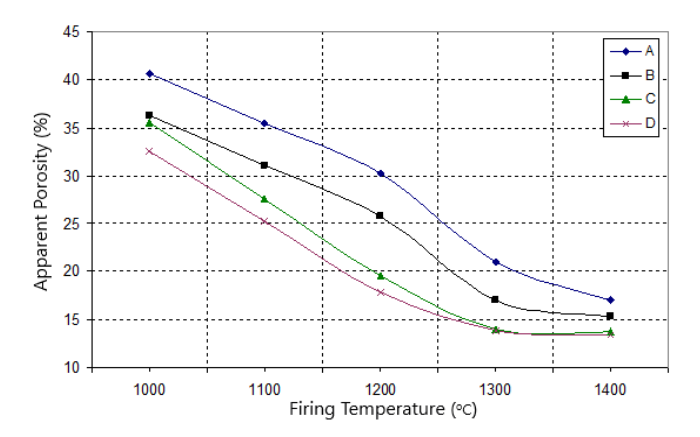


**Figure 12.** The effect of burning temperature on the apparent porosity of the produced specimens

When using the semi-dry-pressing method, the compaction of the particles increases and thus the van der Waals forces between the particles increase [26]. Figure 14 shows the increase in the resistance to shattering with increasing temperature and the percentage of the plasticizer for all

mixtures. The increase in the amount of resistance to shattering is attributed to the increase in the percentage of silicon oxide and aluminum, which play a major role in increasing the percentage of mullite at 1400°C as a result of the chemical reactions between the components of the insulator. Mullite is characterized by mechanical resistance to impact, in addition to the nature of its crystalline structure, which works to increase the bonding strength between the crystals of the produced insulator [7]. From the results, we conclude that mixture (B) at 1400°C represents the best result in resistance to shattering.

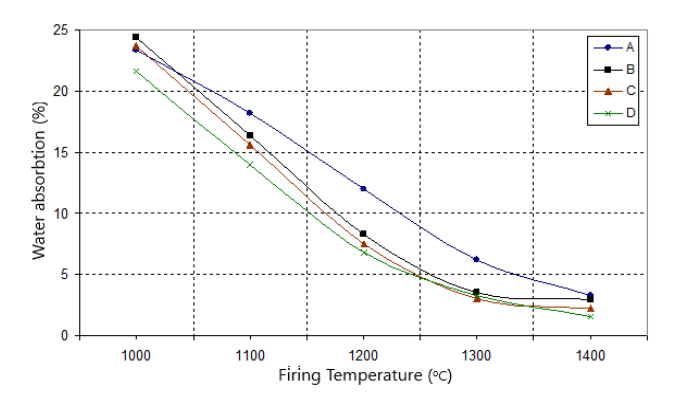


**Figure 13.** The effect of burning temperature on water absorption of the produced specimens

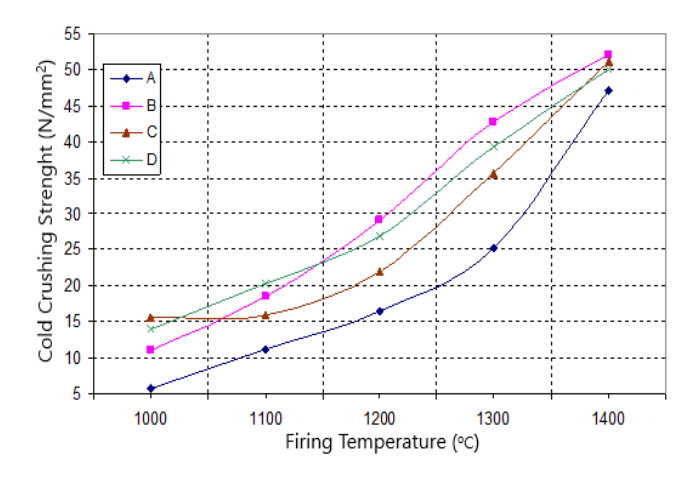


**Figure 14.** The effect of burning temperature on Cold Crushing Strength of the produced specimens

# 3.7 Transient numerical thermal analysis by F.E.M.

Based on the experimental results, the rotary kiln was treated as a practical application. Based on the properties of gases inside the rotary kiln and a set of hypotheses, taking into consideration the best laboratory results for the values of the general properties of the produced refractories ( $\rho$ ,  $C_P$ , k), theories and laws of heat transfer in the unsteady state and steady state were employed by conducting a numerical thermal analysis for each of the coal layer, clinker layer deposited on the inner surface facing the flame, the produced ceramic thermal insulation layer and the metal furnace wall. This was done by simulating the ANSYS program package, in order to reach a design database as a guide for designers of these insulators to choose the best of them with the ideal thickness, reducing effort and costs when dealing practical applications for the industrial sector.

# 3.7.1 Description of the analysis method and hypotheses

The method in its simple form is to calculate the thermal distribution through the composite wall (deposited coal layer, clinker layer, insulating layer, and metal wall) as a function of time [27]. Figure 15 represents the burning area of the rotary kiln, the layer facing the flame is the deposited coal layer and is porous and forms a resistance to heat transfer, and the clinker layer is formed after five hours of operating the rotary kiln, while the ceramic insulating layer under study has a lower temperature due to its lack of direct influence by the flame, in addition to its low thermal conductivity, and finally the metal kiln wall and its weak resistance to heat transfer due to its high thermal conductivity.

In order to address the practical application, a set of hypotheses must be established as follows:

- Neglecting the thermal resistance of the coal layer formed on the inner surface of the combustion zone because it is very small compared to the rest of the resistances.
- The inner surface of the insulating layer is heated instantly to the combustion temperature in contact with the sediment layer, so the thermal resistance of the gas load is neglected, and it is small compared to other thermal resistances.
- The clinker layer is formed on the surface of the insulator in the combustion zone after 5-6 hours from the start of the furnace operation, which adds a new resistance to heat transfer that is taken into account.
- The thickness of the insulating layer does not change before and after combustion.
- The thermal properties (ρ, CP, k) of the layers of the composite rotary kiln do not change with temperature (isotropic), because their chemical composition has great stability and maintains its properties towards high temperatures without changing the performance.
- Heat transfer through the wall of the compound furnace is one-dimensional in radial direction and unststeady state, so that the radius (r) is the only coordinate defining the system, which means that the rate of heat transfer towards the axis of the tube furnace is negligible.
- There is no internal heat generation, i.e. the rate of heat transfer per unit volume is negligible.

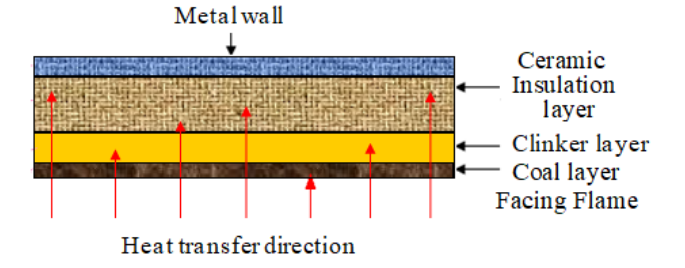


Figure 15. Rotary kiln firing zone layers

**Table 4.** Thermal conductivity as a function of temperature of the mixture (B)

Symbol No.	Burning Temp. (°C)	Bulk Density (g/cm³)	Apparent Porosity (%)	Thermal Conductivity (W/m.°C)
	1000	1.61	36.25	1.2
	1100	1.80	31.02	1.24
В	1200	1.99	25.80	1.28
	1300	2.13	17.00	1.30
	1400	2.17	12.81	1.33

# 3.7.2 Selection of insulators

The insulator subject to the study was chosen according to the encouraging practical results it showed, where mixture (B) consisting of 10% unfired bauxite, 10% kaolinite and 80% grog bauxite was chosen, which exhibited the best thermal and mechanical specifications at temperatures of 1300°C and 1400°C, compared to other mixtures, and its thermal conductivity was measured as in Table 4. Table 5 represents the general specifications of the rotary kiln layers materials under study.

**Table 5.** Rotary kiln layers specifications

Symbol Layer	Symbol No.	Bulk Density (Kg/m³)	Spesific Heat (J/kg.°C)	Thermal Conductivity (W/m.°C)	
$\mathbf{C}$	1	1950	-	2.5	
K	2	2300	850	1.3	
В	3	2030	960	1.33	
M	4	7801	473	43	

#### 3.7.3 Selection initial and boundary conditions

The temperature of 30°C was chosen to represent the initial conditions at which the rotary kiln starts to operate. The boundary conditions were fixed after the kiln started to operate and reached the steady state and they differ according to the kiln zones, which are the preheating zone, calcining zone, firing zone, and final cooling zone. Through a site visit to one of the Iraqi cement factories and reviewing the temperature control data, the kiln was divided into six zones according to the thermal range. The first zone (1600 - 1750°C), the second zone (1150 - 1600°C), the third zone (900 - 1150°C), the fourth zone (450 - 900°C), the fifth zone (200 - 450°C), the sixth zone (30 - 200°C), and Figure 16 represents the rotary kiln zones. The thermal ranges of the second and fourth zones were chosen to be subjected to thermal analysis, and the values for the remaining zones can be deduced based on the results of these two zones. During the thermal analysis, it should be noted that the points of contact of the hot gases with the lining of the inner surface of the oven are used to represent the temperature values of the three zones.

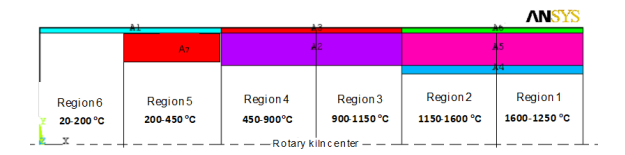


**Figure 16.** Temperature distribution zones for the rotary kiln

# 3.7.4 Building the mathematical numerical model and thermal analysis using ANSYS program

The first stage in the thermal analysis is building the mathematical model that describes the real physical state of the system. The stage includes describing the analysis method, the type of element and its selection (Solid Axisymmetry, Plane 55 2-D, Quad 4 Nodes). In this step, a cross-sectional slice is taken along the rotary kiln in the form of a multi-layer rectangle and by rotating the slice 360 degrees, the final shape of the kiln is formed. Note that the results obtain from the slice give a comprehensive description of the entire system. The physical specifications of the system ( $\rho$ ,  $C_P$ , k) were also fixed and the shape of the system was represented by a drawing (Model Geometry). Finally, the type of node network for the

model (Mesh) was chosen, noting here the use of the smart node network, and Figure 17 gives a clear picture of this method [27]. In the second stage, the thermal load is used and the final solution is obtained, starting with describing the analysis method and then choosing the unsteady state (Eq. (7)) through fixing the initial conditions and until the final solution. The final stage is where the final results are displayed through the program library called (Preprocessor), and the final results are either in the form of charts, values, tables, thermal vectors (Vectors) or layers for distributing heat (Contour).

$$\rho C_{p} \frac{\partial T}{\partial t} = \frac{\partial}{\partial y} \left( k \frac{\partial T}{\partial y} \right) + \dot{q} \tag{7}$$

**Figure 17.** Model of numbering the nodes associated with the analysis method of the ANSYS program

Three case studies were proposed for the second region and a fourth case study for the fourth region as shown in Figure 18. The reason for choosing the second region is that it is exposed to the highest temperature, ranging from (1150-1600°C). The first case study involves the rotary kiln at the beginning of operation and during it until reaching the steady-state, with the thickness of the insulator fixed and the time changed before the clinker layer is formed. The second case study analyzes the second region during operation with the thickness of the insulator fixed and the time changed but after the clinker layer is formed. The third case study analyzes the second region starting from the moment of operation until reaching the steady-state and for different thicknesses of the insulator with the presence of the clinker layer. For comparison with the firing zone, a fourth case study was chosen for the fourth region starting from the moment of operation until reaching the steady-state and for different thicknesses of the insulator. As for the composite kiln wall materials, they were described in Table 5, which showed different thermal and mechanical specifications.

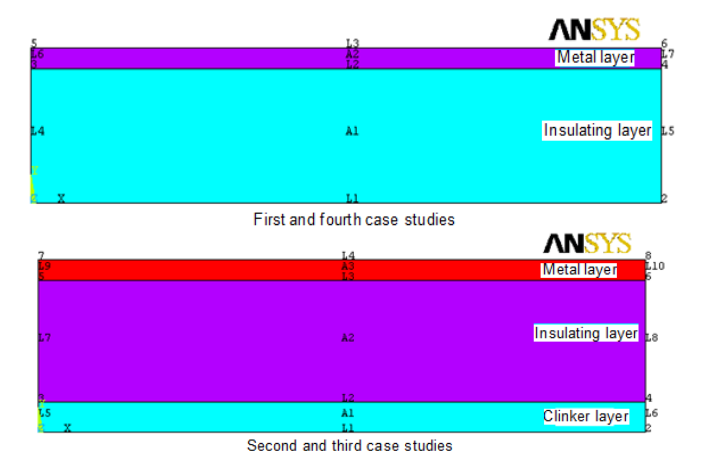
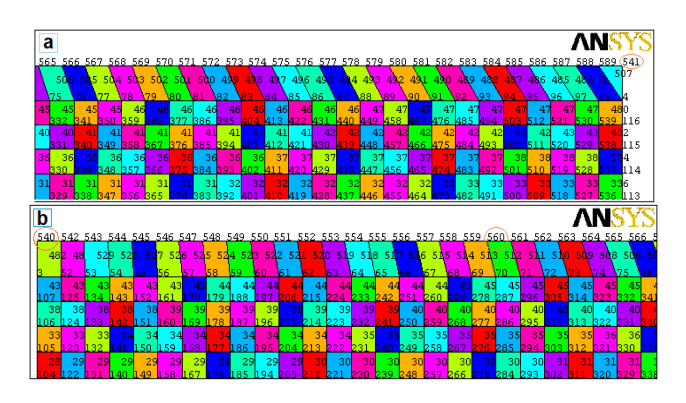


**Figure 18.** Flowchart of proposed case studies for the second and fourth rotary kiln zones

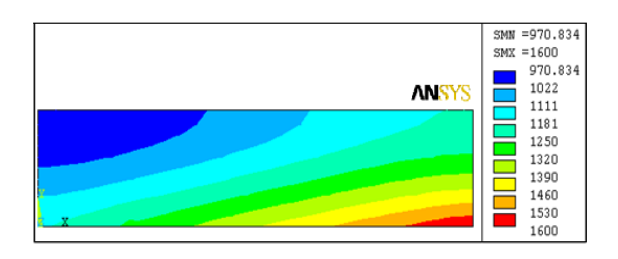
3.7.5 Discussion and comparison of thermal analysis results of case studies

Starting with Case study-1, nodes 541, 560, and 540 were selected on the inner surface of the metal layer of the rotary kiln wall, represented in Figure 19. These nodes represent the points of direct contact with the insulator layer (B) and the metal wall in the second region, starting from the beginning of the flame at a temperature of 1600°C until the end of the second region, where the temperature does not exceed 1150°C. The insulator was selected with a thickness of 15 cm and an operating time starting from the moment of startup until reaching the steady-state, i.e. after 55.5 hours, where it was found that the temperature reaches the steady-state after 45-55 hours. Assuming that the clinker layer is not formed, it was observed that the temperature of the metal surface at node 541 reaches 1250°C compared to node 540, whose temperature reaches 1022°C. The results of the thermal distribution in terms of time and the contour shape are shown in Figure 20. According to the data of the rotary kiln operation in the cement plant, it was found that the safe temperature for the furnace metal is 500°C, and therefore the wall of this area is exposed to high thermal stress, so Case Study-1 cannot be used for insulation.

Case study-2 was proposed, in which the ceramic insulator (B) with a thickness of 20 cm was chosen from the moment the kiln starts up until 55.5 hours.



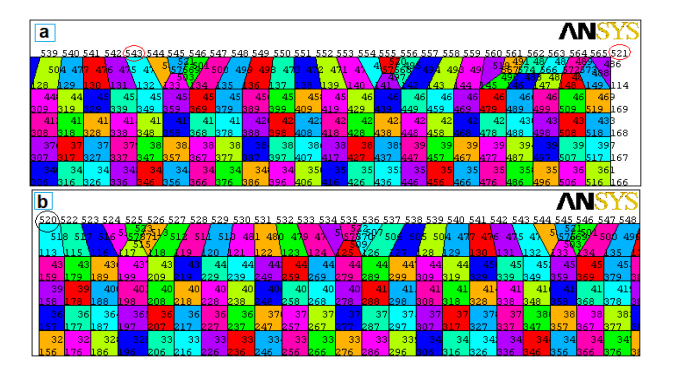
**Figure 19.** Finite Element Method (FEM) node network for Case Study-1, (a) Right side of rotary kiln. (b) Left side of rotary kiln



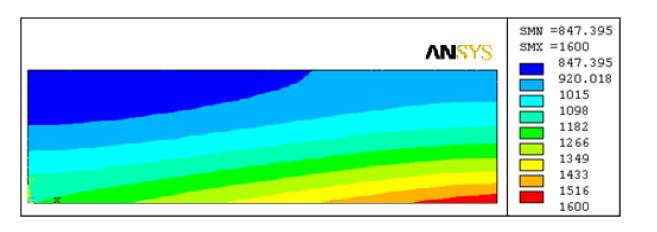
**Figure 20.** The contour form of temperature distribution of the kiln layers is representative of case study -1 after 55.5 hours of starting the rotary kiln for a thickness of 15 cm

A layer of clinker with a thickness of 5 cm is formed, which adds a new resistance to heat transfer as in Figure 18. Since the physical specifications of the clinker are close to the specifications of the ceramic insulator, the total resistance of the two layers (insulator and clinker) with a thickness of 25cm, excluding the thickness of the metal wall. After conducting the numerical thermal analysis of this mathematical model, the results were evaluated at nodes 521, 543, and 520 in Figure 21,

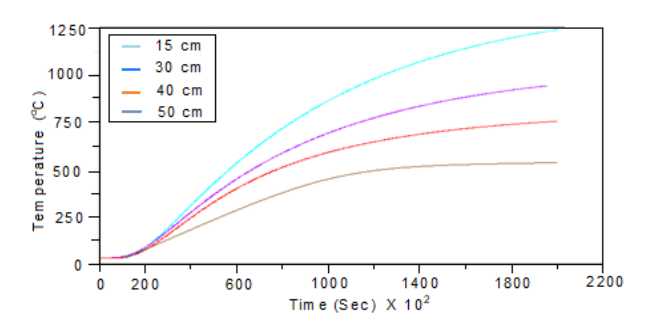
which represents the second region with a temperature range of 1150-1600°C. From Figure 22 of the temperature distribution with time, it was found that the highest temperature was 1015°C at node 521 while the lowest temperature was 847°C at node 520. It can be concluded from the contour form that the furnace wall is still exposed to high thermal stress exceeding the yield point of the metal from which the furnace is made, and therefore, the case study-2 has failed to achieve the purpose of insulation.



**Figure 21.** Finite Element Method (FEM) node network for Case Study-2, (a) Right side of rotary kiln. (b) Left side of rotary kiln



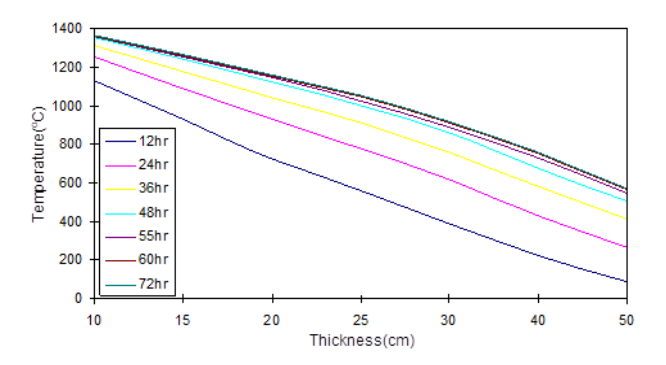
**Figure 22.** The contour form of temperature distribution of the kiln layers is representative of case study -2 after 55.5 hours of starting the rotary kiln for a thickness of 25 cm



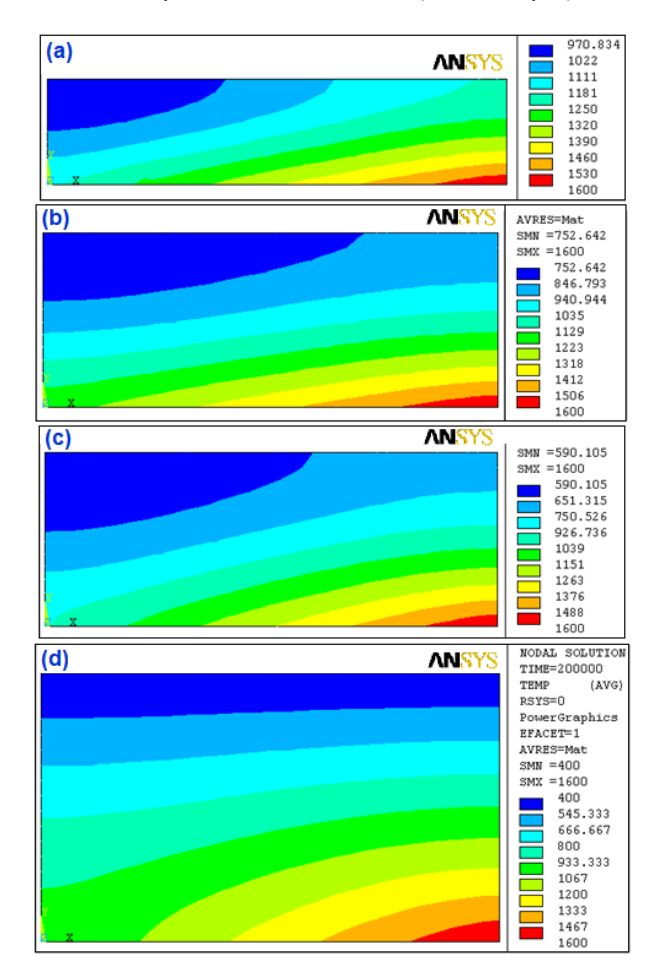
**Figure 23.** Temperature versus time for rotary kiln layers after 55.5 hours of start-up for different thicknesses (Case Study-3)

Case study-3 was proposed starting from the moment of starting the rotary kiln until 55.5 hours and using the same ceramic insulator (B) but with thicknesses of 10, 15, 20, 25, 30, 40, 50 cm including a clinker layer of 5 cm. After evaluating the results through Figures 23 and 24 in the second region of the nodes located on the inner surface of the metal furnace wall which is exposed to the most severe thermal stress. It was found that the temperatures at the beginning of the region for the nodes and the above thicknesses were respectively 545, 651, 940, 1015, 1145, 1250, 1350°C while the temperatures at the end of this region for the previous thicknesses were 400, 590, 752, 847, 900, 970, 1100°C.

What supports the above results is the contour shape of the temperature distribution across the insulator as in Figure 25. It can be concluded that it is not suitable for insulation of the second zone up to a thickness of 50 cm and the furnace wall of this zone is still exposed to high thermal stress approaching the yield point except for greater thicknesses, and this is not economically feasible. Therefore, the insulator described in Case Study-3 is not suitable for insulation.



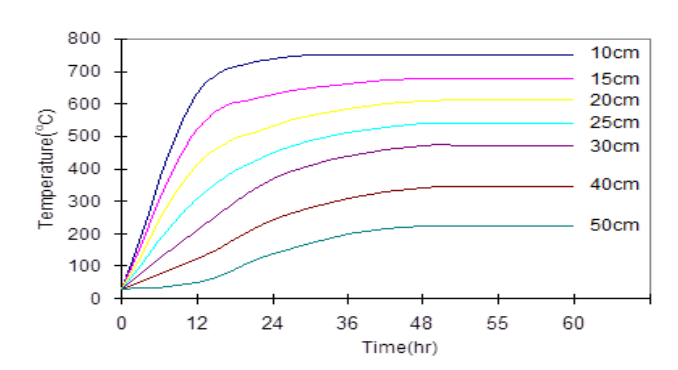
**Figure 24.** Temperatures as a function of thickness of the kilin layers for different times (Case Study-3)



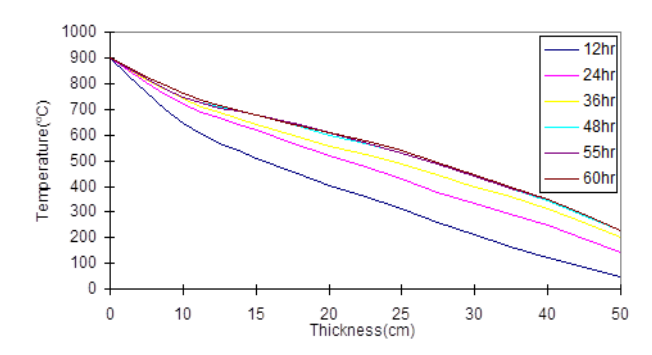
**Figure 25.** The contour form of temperature distribution for case study-3 after 55.5 hours of rotary kiln start-up for different thicknesses of rotary kiln (a) 15 cm (b) 30 cm (c) 40 cm (d) 50 cm

Previous case studies have demonstrated the limitations of using the prepared ceramic insulator in the second zone. Since the rotary kiln consists of six main zones, a new design was considered, represented by **Case Study-4**, through which the

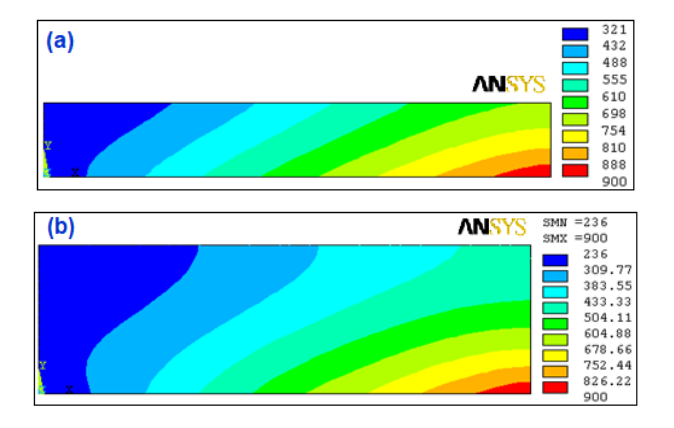
behavior of the insulator in the fourth zone was evaluated between 500 - 900°C using the same time period from the start of the rotary kiln operation until the steady state of 45-55 hours. Different thicknesses were chosen 10, 15, 20, 25,30.40,50 cm, ignoring the clinker layer because it does not form in this zone. Figures 26 and 27 show that the temperatures of the nodes on the front of the inner surface of the kilin were respectively 224. 347, 504, 680, 715, 754, 780°C for thicknesses of (50, 40, 30, 25, 20, 15, 10 cm). While they reach (140, 205, 236, 280, 305, 320, 236)°C for the same thicknesses at the end of the fourth region. By comparing the previous results with the contour shape of the temperature distribution across the insulator as in Figure 28, it was concluded that the insulator with thicknesses of 40 and 50 cm is suitable for completely insulating the fourth region and with a thickness of 30 cm for insulating the second half of this region. As for the thermal range 900-1150°C, by comparing the results of the third and fourth case studies, it can be concluded that a 50 cm thick thermal insulator is suitable for insulating this area safely, as the temperature of the metal wall does not exceed 400°C.



**Figure 26.** Temperature versus time for rotary kiln layers after 55.5 hours of start-up for different thicknesses (Case Study-4)



**Figure 27.** Temperatures as a function of thickness of the kilin layers for different times (Case Study-3)



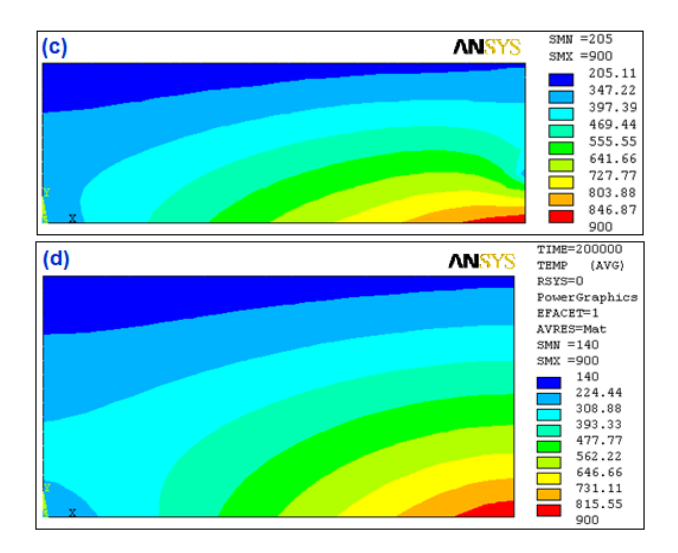


Figure 28. The contour form of temperature distribution for case study-4 after 55.5 hours of rotary kiln start-up for different thicknesses of rotary kiln (a) 15 cm (b) 30 cm (c) 40 cm (d) 50 cm

# 4. CONCLUSIONS

- Chemical examination of the local ceramic raw materials under study proved their suitability for the production of the proposed insulator, due to their high alumina content about 63.02wt% compared to global raw materials.
- XRD analysis results of raw bauxite showed the appearance of kaolinite, boehmite and calcite, while for bauxite burned at 1400°C, mullite was mainly observed with a small percentage of cristobalite, mullite has a high specific gravity of about (3.02) which was reflected in the increase in the specific gravity of the produced refractories.
- Thermal microscope examination and Zecker cone examination showed that the raw materials under study are highly melting refractories, and their softening point is greater than 1600°C, which is equivalent to Zeger Cone 23, the increase in softening point is attributed to the high percentage of alumina in the raw materials about 63.02wt%, as it has a melting point of 2050°C.
- Through differential thermal analysis (DTA) examination, it was possible to determine the endothermic and exothermic reactions, and thus the appropriate burning program was developed.
- The optimum production conditions such as soaking time, firing temperature, plasticizer ratio, and grain size distribution changes on the general properties of the produced samples were determined, and it was found that the samples of mixture (B) were characterized by ideal physical and mechanical specifications, compared to the samples of other mixtures, especially at firing temperatures of 1300°C and 1400°C.
- The numerical mathematical analysis method using ANSYS simulation program gave accurate and clear results in the form of closed graphs and curves for the temperature distribution in the unsteady state that can be adopted by thermal insulator designers to reduce effort and costs and achieve the optimal design.
- From the numerical mathematical analysis, it was found that the prepared ceramic insulators were of limited use and unsuitable for insulating the first and second zones of the

- rotary kiln. While the insulator with a thickness of 50 cm is suitable for insulating the third zone safely.
- The ceramic insulator with thicknesses of 40 and 50 cm is very suitable for insulating the entire fourth zone, where the temperature on the inner metal surface of the oven was between 140-224°C for the thickness of 50 cm, and is considered ideal for the oven wall without reaching the yield point, and with a thickness of 30 cm for insulating the second half of the rotary kiln fourth zone.
- The use of ceramic insulators made of bauxite has several restrictions, including that the furnace temperature does not exceed the permissible limit, mechanical endurance due to its fragility, its ability to absorb moisture, its non-reaction with the chemical media of the materials inside the furnace to avoid corrosion, its service life, and finally the complexity of the design and installation.
- The subsequent study of this study is to improve its properties to enhance its performance at high temperatures and then increase its mechanical resistance against shocks

# ACKNOWLEDGMENT

Thanks and appreciation go to the Department of Chemical Engineering/University of Technology, the University of Baghdad/Department of Science, Al-Quds General Company, Al-Milad General Company and the Geological Survey Department for their support and assistance in making this work a success.

# REFERENCES

- [1] Kingery, W.D. (1989). Ceramic materials science in society. Annual Review of Materials Science, 19(1): 1
  - https://doi.org/10.1146/annurev.ms.19.080189.000245
- [2] Zaidan, S.A, Jasim, H.H. (2017). Effect Nano-SiC additives on physical and mechanical properties of bauxite refractories used in oil treatment units. Engineering and Technology Journal, 35(10 Part A). https://doi.org/10.30684/etj.35.10A.5
- [3] Diko-Makia, L., Ligege, R. (2020). Composition and technological properties of clays for structural ceramics in Limpopo (South Africa). Minerals, 10(8): 700. https://doi.org/10.3390/min10080700
- Rud', R.F., Yutina, A.S., Bulakh, V.L., Zhukova, Z.D. (1981). Effect of some production factors on the life of dinas refractories at high temperatures in reducing conditions. Refractories, 22(7): 429-435. https://doi.org/10.1007/BF01398418
- [5] Nasr, I., Shennawi, E., Messiha, D. (1981). High alumina refractories made of calcined bauxite and synthetic alumina mixtures. Interceram, 30(5): 494-496. http://pascalfrancis.inist.fr/vibad/index.php?action=getRecordDetail &idt=PASCAL82X0028965.
  - Huang, B.Y., McGee, T.D. (1988). Secondary expansion of mullite refractories containing calcined bauxite and calcined clay. American Ceramic Society Bulletin, 67(7): 1235-1238. http://pascalfrancis.inist.fr/vibad/index.php?action=getRecordDetail
    - &idt=6980142.
- Lima, L.K.S., Silva, K.R., Menezes, R.R., Santana, L.N.

- L., Lira, H.L. (2022). Microstructural characteristics, properties, synthesis and applications of mullite: A review. Cerâmica, 68(385): 126-142. https://doi.org/10.1590/0366-69132022683853184
- [8] Ibrahim, S.I., Ali, N.M., Abood, T.W. (2019). Improving the physical and mechanical properties of fireclay refractory bricks by added bauxite. Journal of Engineering, 25(4): 18-28. https://doi.org/10.31026/j.eng.2019.04.02
- [9] Khanmohammadi, S., Mohtadinia, M. (2024). High temperature corrosion resistance of various aluminosilicate refractory bricks. Ceramics International, 50(23): 49125-49133. https://doi.org/10.1016/j.ceramint.2024.09.254
- [10] Shackelford, J.F., Doremus, R.H. (2008). Ceramic and Glass Materials. Structure, Properties and Processing. Springer. https://doi.org/10.1007/978-0-387-73362-3
- [11] Al-Amaireh M. (2006). Improving the physical and thermal properties of the fire clay refractory bricks produced from bauxite. Journal of Applied Sciences, 6(12): 2605-2610. https://doi.org/10.3923/jas.2006.2605.2610
- [12] Al-Amer, E.M.H., Al-Kadhemy, M.F.H. (2015). Improving the physical properties of Iraqi bauxite refractory bricks. Al-Nahrain Journal of Science, 18(3): 67-73. https://doi.org/10.22401/JNUS.18.3.10
- [13] Hussein, H. (2019). Improve some properties of refractory mortar manufactured from grog bauxite, attapulgite, CaO and white cement by using Gum Arabic. International Journal of Civil Engineering and Technology, 10(3): 155-166. https://iaeme.com/MasterAdmin/Journal\_uploads/IJCIE T/VOLUME 10 ISSUE 3/IJCIET 10 03 127.pdf.
- [14] Harith, I.J., Hani, M.H. (2017). Study the physical properties of refractory mortar contains kaolin—metakaoline—fire brick powder—sic. International Journal of Chemtech Research, 10(9): 790-799.
- [15] Al Hwaidy, K.E., Hassan, S.S., Eedan, O.A. (2018). Study the effect of using local materials as refractory bonding mortar in Iraqi. Kufa Journal of Engineering, 9(1): 143-157.
- [16] Zaidan, S.A., Omar, M.H. (2018). The effects of bauxite, metakaolin, and porosity on the thermal properties of prepared Iraqi clays refractory mortars. Applied Physics A, 124(5): 386. https://doi.org/10.1007/s00339-018-1759-2
- [17] Xu, L., Zhang, D., Liu, Y., Chen, M., Wang, N. (2021). Comparison of microstructure, thermo-mechanical property and corrosion resistance of bauxite-corundum refractory castables reinforced by two approaches. Ceramics International, 47(10): 13660-13668. https://doi.org/10.1016/j.ceramint.2021.01.227
- [18] Mebrek, A., Rezzag, H., Ladjama, S., Azzi, A., Grairia, A., Taibi, Y. (2023). Development of composite ceramics with kaolin and spent refractory bricks. JOM, 75(12): 5808-5818. https://doi.org/10.1007/s11837-023-06203-9
- [19] Callister Jr, W. D., & Rethwisch, D. G. (2020). Materials science and engineering: an introduction. John wiley &
- [20] Eissa, A., Ghazy, A., Bassuoni, M.T., Alfaro, M. (2021). Improving the properties of soft soils using nano-silica, slag, and cement. In Proceedings of the 6th World Congress on Civil, Structural, and Environmental

- Engineering (CSEE'21), Virtual Conference, No. ICGRE 101. https://doi.org/10.11159/icgre21.lx.101
- [21] ASTM C133–97. (2015). Standard test methods for cold crushing strength and modulus of rupture of refractories. Am. Stand. Test Methods.
- [22] Boccaccini, D. N., Romagnoli, M., Kamseu, E., Veronesi, P., Leonelli, C., Pellacani, G.C. (2007). Determination of thermal shock resistance in refractory materials by ultrasonic pulse velocity measurement. Journal of the European Ceramic Society, 27(2-3): 1859-1863. https://doi.org/10.1016/j.jeurceramsoc.2006.05.070
- [23] Pilling, M.W., Yates, B., Black, M.A., Tattersall, P. (1979). The thermal conductivity of carbon fibrereinforced composites. Journal of Materials Science, 14: 1326-1338. https://doi.org/10.1007/BF00549304
- [24] Cruz, M.D.R., Franco, F. (2000). Thermal behavior of the kaolinite-hydrazine intercalation complex. Clays and Clay Minerals, 48(1): 63-67. https://doi.org/10.1346/CCMN.2000.0480108
- [25] Ohring, M. (1995). Engineering Materials Science (Vol. 3). Academic press.
- [26] Smait, D.A., Mohammed, F.M., Al-Falahi, H.A., Alwan, H.L., Alani, S. (2023). Analysis of impact loading response on the composites materials as a function of graphite filler content using Taguchi method. Revue des Composites et des Matériaux Avancés-Journal of Composite and Advanced Materials, 33(2): 121-125. https://doi.org/10.18280/rcma.330207
- [27] Al-Falahi, H.A. (2023). Thermal analysis and modification of C/C ablative composites for high-temperature insulation applications. Revue des Composites et des Matériaux Avancés-Journal of Composite and Advanced Materials, 33(6): 379-391. https://doi.org/10.18280/rcma.330605

# **NOMENCLATURE**

$L_1$	Sample height before burning, cm
$L_2$	Sample height after burning, cm

 $\rho$  Bulk density, (g/cm<sup>3</sup>).

W<sub>D</sub> Sample weight after burning, g V Sample volume, after burning, cm<sup>3</sup>

 $V_t$  Total volume of the sample, cm<sup>3</sup>  $V_s$  Volume of the solid fraction cm<sup>3</sup>

V<sub>P</sub> Volume of pores, cm<sup>3</sup>

Q Porosity, %

 $W_{\%}$  Water absorbtion, %

 $W_S$  Weight of the burned sample saturated with  $H_2O$ , g

T Specific gravity

S Cold Crushing Strength, N/mm<sup>2</sup>

F Force, N

A Cross sectional area of sample. mm<sup>2</sup>

RBW Refractory brick waste FEM Finite Element Method XRD X-ray diffraction

HMT Heating microscopy test
DTA Differential thermal analysis

Testing of ceramic materials (German Language:

DIN Deutsches Institut für Normung)

ASTM American standared for testing materials

# Greeksymbols

- α
- Thermal diffusivity,  $m^2$ .  $s^{-1}$  Density,  $Kg.\ m^{-3}$  Thermal conductivity,  $W.m^{-1}.\ k^{-1}$  $\begin{array}{c} \rho \\ k \end{array}$